High-fat diet-induced obesity accelerates the progression of spontaneous osteoarthritis in Senescence-Accelerated Mouse Prone 8 (SAMP8)

Chenyang Ding[1], Dilimulati Yimiti[1], Yohei Sanada[1, 2], Yuki Matsubara[1], Tomoyuki Nakasa[3], Kiminori Matsubara[4], Nobuo Adachi[1] and Shigeru Miyaki[1, 2#]

[1] Department of Orthopaedic Surgery, Graduate School of Biomedical & Health Sciences, Hiroshima University, Hiroshima, Japan.

[2] Medical Center for Translational and Clinical Research, Hiroshima University Hospital, Hiroshima, Japan.

[3] Department of Artificial Joints and Biomaterials, Graduate School of Biomedical and Health Sciences, Hiroshima University, Hiroshima, Japan.

[4] Department of Human Life Science Education, Graduate School of Education, Hiroshima University, Higashi-Hiroshima, Japan

[#]Correspondence to: Shigeru Miyaki, Ph.D.

Medical Center for Translational and Clinical Research, Hiroshima University Hospital, 1-2-3 Kasumi Minami-ku Hiroshima 734-8551, Japan

TEL: +81-82-257-5233 FAX:+81-82-257-5234

E-mail: miyaki@hiroshima-u.ac.jp

Abstract

Objectives: Aging and obesity are major risk factors for osteoarthritis (OA), a widespread disease currently lacking efficient treatments. Senescence-accelerated mouse prone 8 (SAMP8) display early-onset aging phenotypes, including OA. This study investigates the impacts of high-fat diet (HFD)-induced obesity on OA development in SAMP8.

Methods: SAMP8 at five weeks were fed either a normal chow diet or an HFD for ten weeks to induce obesity. Parameters related to obesity, liver function, and lipid and glucose metabolism were analyzed. At 14 weeks of age, knee joint pathology, bone mineral density, and muscle strength were assessed. Immunohistochemistry and TUNEL staining were performed to evaluate markers for cartilage degeneration and chondrocyte apoptosis.

Results: At 14 weeks of age, HFD-induced obesity increased liver and adipose tissue inflammation in SAMP8 without further exacerbating diabetes. Histological scoring revealed aggravated cartilage, menisci deterioration, and synovitis, while no further loss of bone mineral density or muscle strength was observed. Increased chondrocyte apoptosis was detected in knee joints following HFD feeding.

Conclusions: Ten weeks of HFD feeding promotes spontaneous OA progression in 14-week-old SAMP8, potentially via liver damage subsequent chondrocyte apoptosis. This aging-obese mouse model may prove valuable for further exploration of spontaneous OA pathophysiology.

Keywords: Apoptosis, High-fat diet, Obesity, Osteoarthritis, SAMP8

Introduction

Osteoarthritis (OA), the most prevalent joint disease that affects millions of people worldwide, is characterized by the loss of cartilage and bone remodeling, leading to pain, stiffness, and loss of mobility[1]. While OA can affect nearly any joint in the body, it predominantly occurs in weight-bearing joints, such as the hips and knees[2]. As a multifactorial disorder, spontaneous OA is initiated and perpetuated by a complex interplay of various contributing factors. Aging and obesity have been identified as significant risk factors for OA, because the risk of developing OA increases with age and overload, as the joints are subjected to years of wear and tear. The increased pressure on weight-bearing joints from carrying excess weight can cause inflammation and cartilage damage. Moreover, obesity is linked to chronic low-grade inflammation, which may further contribute to OA development[3]. In human OA cases, aging and obesity often cooperatively contribute to the progression of OA, imposing a substantial burden on healthcare systems[4], especially with the background of expanding elderly population in many countries.

Senescence-accelerated mouse (SAM), is a mouse strain derived from the AKR/J strain[5]. SAM consists of senescence-prone inbred strains (SAMP) and senescence-resistant inbred strains (SAMR) line which shows normal aging characteristic[5]. Thus, in SAM studies, SAMR has been used as control of SAMP. Among SAMP, SAMP8 has been used as a mouse model to investigate aging-related neurological and cognitive

deficits, such as Alzheimer's disease[6]. In C57BL/6 mice, moderate OA-like changes become detectable at 12-24 months, at least[7, 8]. However, we recently reported that SAMP8 exhibited significant meniscus and cartilage degeneration in knee joints with subchondral bone sclerosis and osteopenia from an early stage of about 14 weeks of age[9]. Furthermore, although various studies have examined the relationship between obesity and OA in ob/ob mouse, diet-induced obese C57BL/6 mice and/or post-traumatic OA models[10, 11, 12, 13, 14], the potential influence of obesity on the accelerated aging-related primary OA and the underlying mechanisms have yet to be determined. The purpose of the present study was to determine the effect of high-fat diet (HFD)-induced obesity to the development of OA in spontaneous OA model mouse, SAMP8.

In the present study, we demonstrated that in SAMP8, high-fat diet-induced obesity induces liver damage and further aggravates the severity of primary OA at an early age of 14 weeks through increased chondrocyte apoptosis, without further exacerbating remarkable metabolic dysregulation such as hyperlipidemia and diabetes.

Materials and Methods

Animal Model and Experimental Design

SAMP8 at 4 weeks of age were obtained from Japan SLC (Shizuoka, Japan), and only male mice were used in this study. After one week of acclimatization, forty SAMP8 were randomly divided into two groups: the high-fat diet (HFD) group (n=20) and the

normal chow diet (ND) group (n=20). The HFD group was fed a diet of HFD-60 (Protein:Fat:Carbohydrate = 18.2:62.2:19.6, Oriental Yeast Co., Ltd., Tokyo, Japan) for 10 weeks, while the ND group was fed a normal chow diet (AIN93M; Protein:Fat:Carbohydrate = 14.1:10.0:75.9, Oriental Yeast) (Fig. 1A). All mice were housed in groups of five per cage (S143 mm × 293 mm × H148mm) with a sterilized beta-chip bedding and maintained at 23±1 °C with a 12-h light/dark cycle and acidified water and complete commercial pelleted food ad libitum. Body weight was measured weekly. Mice were sacrificed for histological and biological analyses at 14 weeks of age. All animal experiments were performed according to protocols approved by the Hiroshima University Animal Care and Use Committee.

Histopathological Assessments of Knee Joints

Knee joints from each mouse were embedded intact in paraffin after fixation in 4% paraformaldehyde phosphate buffer solution (PFA-PBS) for 48h at 4°C and decalcification in K-CX (FALMA, Japan) for 6 h at room temperature. Paraffin-embedded knee joints were sectioned at 4.5 μm in the coronal plane through the central weight-bearing region of the anterior and posterior femorotibial joint. Three different sections per joint were stained with Safranin O (MUTO PURE CHEMICALS, Tokyo, Japan) and Fast Green (Sigma-Aldrich, USA). Histological assessments were performed on each section, and the average scores from three different sections were used for statistical analysis. Three different researchers were blinded while performing

all scorings. Scoring systems for articular cartilage, meniscus, subchondral bone, and synovium were applied in this study. Damage of articular cartilage (maximum 24 points per knee joint section; 6 points for each quadrant of the medial and lateral femoral/tibial cartilage) was evaluated using the OARSI scoring system [15]. Subchondral bone changes, meniscus degradation, and the severity of synovitis were evaluated according to previously described histopathological scoring systems[16, 17, 18] using the left knee joints.

Hematoxylin and Eosin (H&E) Staining

The liver, epididymal and subcutaneous fat tissue were resected from mice and immediately fixed in 4% PFA-PBS. The tissues were embedded in paraffin and sliced into 4.5μm thick sections for H&E staining. Slides were imaged using a Keyence BZ-X800 microscope (Keyence Cooperation, Japan). The H&E-stained sections of the epididymal adipose tissue were analyzed for adipocyte size determination and crown-like structures (CLS) quantification using Image J software (NIH, USA).

Blood Biochemical Analysis

Blood samples were collected by cardiac puncture after sacrifice. After coagulating at room temperature for one hour, the blood samples were centrifuged under 1,500g for 30 min. Supernatant serum were collected for subsequent analyses. Serum biomarkers of aspartate aminotransferase (AST), alanine aminotransferase (ALT), total

128 cholesterol (T-CHO), triglycerides (TG), glucose (GLU) and non-esterified fatty acid
129 (NEFA) in serum were analyzed by Nagahama Life Science Laboratory (Nagahama,
130 Japan) using routine laboratory methods.
131
132 **Glucose Tolerance Test (GTT)**
133 See Supplemental Materials.
134
135 **Dual-energy X-ray Absorptiometry (DEXA) Analysis**
136 See Supplemental Materials.
137
138 **Grip Strength Test**
139 See Supplemental Materials.
140
141 **TUNEL Staining**
142 TUNEL staining was completed using an in-situ detection kit for programmed cell death
143 detection (MEBSTAIN apoptosis TUNEL Kit direct: MBL, United States) according to
144 the manufacturer's instructions. Nuclei were stained by 4′,6-diamidino-2-phenylindole
145 (DAPI).
146
147 **Immunohistochemical Analysis**
148 Slides were pretreated with antigen-retrieval reagent (Immunoactive; Matsunami Glass

149 Ind, Osaka, Japan) at 60°C for 16 hours, followed by blocking serum for 30 minutes.
150 Then, sections were immunostained with anti-C/EBP homologous protein (CHOP)
151 antibody (proteintech, 15204-1-AP, 3.5μg/mL), anti-p16^{INK4a} antibody (abcam, ab54210;
152 0.1μg/mL), anti-ADAMTS5 antibody (GeneTex, GTX100332, 10μg/mL) and anti-
153 MMP13 antibody (ThermoFisher Scientific, MA5-14328, 20μg/ml) diluted in Can Get
154 Signal immunostaining solution (TOYOBO, Tokyo, Japan) using Vectastain Elite ABC-
155 HRP kit and DAB substrate kit (Vector Laboratories, Burlingame, CA, USA) according
156 to the manufacturers' instructions.
157

158 **Statistical Analyses**

159 Data are expressed as mean ± standard deviation or median ± 95% confidence interval
160 (knee histopathological scores). Statistical analysis of data was performed using Prism
161 v9.5.1 (GraphPad Software, San Diego) as follows: two-tailed unpaired Welch's t tests
162 for tissue weights, blood biochemical markers, muscle strength and quantifications of
163 histological data; 2-way ANOVA with Sidak's multiple correction for body weight;
164 nonparametric Mann-Whitney tests for knee histopathological scores; multiple
165 unpaired t tests with Holm-Sidak's multiple correction for bone mineral density. The
166 results were considered statistically significant at a value of $p < 0.05$.
167

168 **Results**

169 **High-fat diet feeding induced obesity in SAMP8**

170 To assess the impact of a high-fat diet (HFD) on the body weight of SAMP8 in
171 comparison to a normal chow diet (ND), we monitored the body weight of mice from
172 both groups on a weekly basis. The body weight of the HFD group was significantly
173 increased compared to the ND group (Fig. 1B, C). The average increase in body weight
174 was 5.228 grams at 14 weeks of age. Furthermore, we observed an increase in the
175 tissue weight of the liver (Fig. 1D), as well as epididymal and subcutaneous fat (Fig.
176 1E). These results demonstrate that 10 weeks of HFD feeding, from 5 to 14 weeks of
177 age, induced obesity and increased fat accumulation in SAMP8.
178

179 **Lipid and glucose metabolism in SAMP8 by HFD**

180 Given the observed increase in liver and fat tissue weights in the HFD-fed mice, we
181 investigated the effects of HFD on function of liver and adipose tissue next, as well as
182 lipid and glucose metabolism, as obesity is a significant predisposing factor for
183 metabolic dysregulation, such as non-alcoholic fatty liver disease (NAFLD),
184 hyperlipidemia and type 2 diabetes. We observed enlarged hepatocytes and an
185 increased number of lipid droplets in the livers of HFD-fed mice compared with those
186 fed with a chow diet, as seen in the H&E-stained sections (Fig. 2A). Liver damage
187 markers, aspartate aminotransferase (AST) and alanine aminotransferase (ALT), were
188 significantly upregulated in the HFD group (Fig. 2B). Circulating lipids, including TG
189 and T-CHO significantly reduced in serum of HFD group, indicating liver inflammation
190 and damage induced by the HFD (Fig. 2C). Moreover, the HFD group exhibited

191 reduced serum albumin concentration and albumin/globulin (A/G) ratio, and
192 unchanged total protein levels (Supplemental Fig. 1A), while the renal function markers
193 were unaltered (Supplemental Fig 1B), suggesting an impaired hepatic function in
194 these mice. Additionally, serum ammonia (NH_3) levels were found to be elevated in the
195 HFD group (Supplemental Fig. 1C), further supporting the notion of impaired liver
196 function and ammonia clearance due to the HFD. Furthermore, to assess the influence
197 of HFD on adipose tissue morphology and inflammation, we analyzed H&E-stained
198 microscopic images of epididymal adipose tissue. Adipocyte size (Fig. 2D and E) and
199 crown-like structure (CLS) ratio (Fig. 2F) were increased in the HFD group, indicating
200 increased macrophage infiltration and systemic predisposition to inflammation[19, 20].
201 Although 8 out of 20 SAMP8 in the ND group already displayed an impaired clearance
202 of blood glucose and hyperglycemia (>150mg/dL) (Fig. 2G and H) at 14 weeks, HFD
203 feeding did not further exacerbate the signs of diabetes mellitus, as demonstrated by
204 the intraperitoneal glucose tolerance test (iGTT) (Fig. 2G) and fasting glucose levels,
205 as well as non-esterified fatty acid (NEFA) levels (Fig. 2H). These results indicated that
206 HFD led to liver and adipose tissue inflammation, as well as liver damage, in SAMP8.
207 However, within the study timeframe, HFD did not cause considerable exacerbation of
208 hyperlipidemia or diabetes mellitus.
209

210 **Evaluation of knee pathological changes in HFD- and ND-fed SAMP8**

211 To determine whether HFD promotes the OA-like knee joint changes in SAMP8, we

212 assessed the histopathological changes in the knee joints of these mice using
213 Safranin-O and Fast Green staining. At 14 weeks of age, the HFD group exhibited
214 reduced Safranin-O staining, indicating proteoglycan loss, roughened surface, or
215 cartilage erosion, which in turn indicate more severe cartilage loss compared to the
216 ND group (Fig 3A a and e). The OARSI score revealed a significant elevation in the
217 HFD group (Fig. 3B). OA severity was markedly increased in the medial compartment
218 compared with the lateral compartment (Fig. 3C). Moreover, structural destruction of
219 the medial menisci is a characteristic appearance during OA progression, which
220 displayed even prior to the cartilage degeneration, according to our previous findings[9].
221 The deterioration of medial menisci was more severe in the HFD group (Fig 3A b and
222 f), as determined by the meniscus score (Fig. 3D), while the scores of lateral menisci
223 in both groups remained at the same low level. Synovitis, which is commonly
224 associated with OA, was significantly aggravated in the HFD group according to the
225 synovitis scores (Fig. 3A c and g, Fig. 3E). Furthermore, both groups exhibited
226 complete sclerotic changes, i.e., bone-bone marrow replacement at medial tibial
227 subchondral bone (Fig. 3A d and h). The subchondral bone scores plateaued at 14
228 weeks of age (Fig. 3F), which are consistent with our previous findings[9].
229 These results indicate that HFD-induced obesity accelerates cartilage and medial
230 meniscus deterioration, as well as synovitis in 14-week-old SAMP8, suggesting a
231 worsening of OA status due to the HFD.
232

233 **Bone density and muscle strength in HFD-fed SAMP8**

234 Osteoporosis and sarcopenia, not only OA, are common and significant age-related
235 diseases of the musculoskeletal system in human, and appear earlier in SAMP8[9, 21].
236 Thus, we assessed their bone density and muscle strength. Although SAMP8 already
237 exhibited significantly low BMD in femur compared with SAMR1 at 9 weeks of age[9],
238 HFD-fed SAMP8 had no further decline in bone density compared with ND-fed SAMP8
239 at 14 weeks of age (Fig. 4A). Additionally, grip strength test did not show any early-
240 onset of muscle strength decrease in HFD-fed SAMP8 (Fig. 4B). Therefore, these
241 results suggested that obesity by HFD feeding did not exacerbate the phenotypes of
242 osteoporosis or sarcopenia in SAMP8 at 14 weeks.

243

244 **Molecular mechanisms of HFD-induced OA progression in SAMP8**

245 To further elucidate the underlying mechanisms through which HFD-feeding
246 exacerbates OA-like changes in SAMP8, we conducted a series of in situ detection
247 focusing on potential molecular markers. Chondrocyte apoptosis has been reported to
248 be induced by HFD through induced endoplasmic reticulum (ER) stress[22, 23], which
249 strongly associates with cartilage degradation and OA[24], so we performed TUNEL
250 staining to detect apoptotic chondrocytes. Our results revealed that SAMP8 subjected
251 to 10 weeks of HFD feeding exhibited an increased number of apoptotic chondrocytes
252 in their knee articular cartilage (Fig. 5A) , which was accompanied by a significant
253 upregulation of C/EBP homologous protein (CHOP) (Fig. 5B), a mediator of ER-stress-

254 induced apoptosis[22]. We also assessed the expression of $p16^{INK4a}$, a cell cycle
255 regulator and a marker of chondrocyte senescence[25] that we previously found to be
256 upregulated in SAMP8 compared to SAMR1. Immunohistochemistry analysis
257 demonstrated that the rates of $p16^{INK4a}$-positive chondrocyte remained unchanged in
258 SAMP8 cartilage after HFD feeding (Fig. 5C). Additionally, we examined the
259 expression of MMP13 and ADAMTS5, two hallmark metalloproteinase genes that are
260 involved in cartilage degradation. However, immunohistochemical staining revealed no
261 significant differences in the expression of these genes between the HFD and ND
262 groups (Fig. 5D and E).

263 These results suggested that the increased severity of OA-like changes in HFD-fed
264 SAMP8 may be primarily attributed to the elevated rate of chondrocyte apoptosis, while
265 the expression levels of cellular senescence marker $p16^{INK4a}$ and cartilage degradation
266 markers, MMP13 and ADAMTS5, appear to be unaffected by HFD feeding.

267

268 **Discussion**

269 OA is a heterogenous disorder, while aging is recognized as the predominant risk
270 factor contributing to its development and progression. Nonetheless, at present, many
271 studies utilize post-traumatic mouse OA models, such as destabilization of the medial
272 meniscus (DMM), or rely on naturally aging mice, which require more than about 12
273 months to induce OA-like changes[7, 8]. In our recent study, we demonstrated that the
274 SAMP8 displays knee OA-like changes, and bone density loss in femur, at an early

275 age (14 weeks of age)[9]. Obesity represents another significant risk factor for OA and
276 frequently coexists with aging. The combined effects of obesity and aging not only
277 exacerbate OA through cumulative wear and tear on joints but also contribute to
278 increased levels of inflammation[3]. In the present study, to unveil the combined effect
279 of HFD-induced obesity and aging, we subjected SAMP8 to HFD feeding for 10 weeks,
280 and found that HFD-induced obesity further exacerbates the OA in SAMP8 through
281 elevated apoptosis. Thus, we suggest that SAMP8 serves as a valuable model for
282 studying molecular mechanisms and developing preventive or therapeutic approaches
283 for aging-related musculoskeletal diseases, particularly OA, because SAMP8
284 spontaneously exhibits OA manifestations as early as 14 weeks of age which can be
285 useful for evaluating the pathogenesis of OA influenced by various factors, such as
286 HFD.

287 In the body parameters of ND- and HFD-fed SAMP8, after 10 weeks of feeding from
288 5-week-old, the body, liver, and fat tissue weight of mice in the HFD group were
289 significantly higher than those in the ND group. The difference in body weight (HFD:
290 34.52g vs ND: 29.29g, +17.8%) meets the criteria for obesity (15%) according to
291 previous research[26], and which is comparable with previous studies[27, 28]. The
292 weight gains induced by HFD exacerbated the severity of OA in 14-week-old SAMP8.
293 According to our previous study, compared to SAMR1, SAMP8 exhibited significant
294 meniscal damage at 11 weeks and cartilage damage at 14 weeks, with early sclerosis
295 of subchondral bone already present at 6 weeks[9]. In the present study, we compared

296 the cartilage damage in the knee joints by OARSI score, and SAMP8 fed with HFD
297 displayed a more severe cartilage loss. OA severity was markedly increased in the
298 medial compartment. Moreover, structural destruction of the menisci was observed,
299 which, based on previous studies, could be due to mechanical damage resulting from
300 increased weight load[29]. We also showed that increased levels of synovitis in the
301 joints were consistent with the elevated inflammation levels observed in adipose tissue;
302 however, this could also be a consequence of cartilage damage and repair[30],
303 because synovitis was exhibited after cartilage degradation. In addition, the sclerosis
304 of the subchondral bone in both groups already reached a plateau at 14 weeks of age,
305 in line with our earlier observations[9]. Thus, HFD-induced obesity may promote the
306 severity of OA in SAMP8 through locally overloading in medial compartment.
307 Furthermore, we examined other age-related musculoskeletal disorders. Osteoporosis
308 is an important aging-related phenotype in human and mouse, but its relationship with
309 obesity is complex. Obesity increases bone density through elevated mechanical
310 load[29], while on the other hand, enhances bone resorption through systemic
311 inflammation by cytokines such as TNF-a and IL-6[31, 32]. In comparison to SAMR1,
312 SAMP8 have a significantly more severe bone loss in femur at an early age of 9
313 weeks[9]. However, at 14 weeks, our DEXA data revealed that HFD did not further
314 decrease bone density, because bone loss already reached a plateau at 9 weeks of
315 age[9]. Thus, the interplay between mechanical and inflammatory factors, along with
316 the intrinsic properties of SAMP8 strain, results in the unaltered bone density loss in

317 HFD-SAMP8.

318 Sarcopenia is another prevalent aging-related condition, characterized by
319 progressive deterioration in skeletal muscle functions and loss in mass[33]. The
320 biomechanical effect resulting from cross-talk of joints and periarticular muscle could
321 be associated with the development of OA. The prevalence of sarcopenia in people
322 with knee OA was 45.2%, the prevalence of sarcopenia in knee OA was more than two
323 times higher than in the control group[34]. SAMP8 exhibits sarcopenia around 35
324 weeks of age[21]. At 14 weeks of age, however, HFD-SAMP8 did not exhibit
325 acceleration of the early onset of sarcopenia. Thus, in SAMP8, muscle
326 strength/sarcopenia might not be an initiator of OA.

327 SAMP8 exhibits severe liver damage compared with SAMR1[35]. Furthermore, HFD-
328 induced obesity in C57BL/6 or SAMP8 leads to metabolic disorders such as NAFLD,
329 hyperlipidemia and hyperglycemia[36, 37, 38], which are strongly associated with OA
330 and may predispose the body to an OA-prone environment through shared
331 mechanisms of inflammation, oxidative stress, common metabolites and endothelial
332 dysfunction[39, 40]. In the present study, although HFD-fed SAMP8 did not exhibit
333 further exacerbation of diabetic changes, adipose tissue inflammation and NAFLD-like
334 liver damage were identified. The phenotype could be attributed to the relatively short
335 timeframe of the study (10 weeks), as HFD typically induces hyperglycemia in at least
336 12 weeks[41]. However, NAFLD resulted in hepatic and systemic
337 hyperammonemia[42], concordant with our findings in the present study that HFD-

338 SAMP8 with NAFLD and impaired hepatic function, exhibit elevated blood ammonia
339 levels. Reduced TG and T-CHO in HFD group may indicate more severe liver damage
340 by the HFD in SAMP8. Thus, NAFLD might be a potential mechanism of accelerated
341 severity of OA in HFD-fed SAMP8. We should further examine the relation between
342 liver damage and OA pathogenesis because these results might open a new insight in
343 mechanisms of OA through NAFLD.

344 A marker of dysfunctional senescent cell including chondrocytes, $p16^{INK4a}$, is a cell
345 cycle inhibitor[25]. In our recent study, $p16^{INK4a}$ expression increased in SAMP8 at 6,
346 9, and 11 weeks, indicating accelerated chondrocyte senescence in these[9]. In other
347 OA-related studies, suppressing $p16^{INK4a}$ or clearance of $p16^{INK4a}$-positive
348 chondrocytes suppress OA[43, 44]. On the other hand, there are reports suggesting
349 that the expression of $p16^{INK4a}$ does not contribute to the development of OA[25]. In
350 our results, no differences were observed between the two SAMP8 groups, indicating
351 that modulation of $p16^{INK4a}$ expression is not the way that HFD participate in OA
352 pathogenesis. Moreover, MMP13 and ADAMTS5 are two of the most prominent
353 metalloproteinases directly involved in the degradation of cartilage extracellular matrix
354 components, regulated by upstream factors such as inflammation-related NF-κB
355 pathway[45, 46]. However, in our study, we did not observe any significant changes in
356 these two enzymes, suggesting that inflammation is not the primary factor for HFD-
357 induced OA. Thus, HFD-induced obesity did not upregulate the local inflammatory
358 condition in various tissues/cells of knee joint such as articular chondrocytes and may

359 not be strongly associated with the upregulation of ADAMTS5 and MMP13. The
360 present study indicated the potential role of chondrocyte apoptosis in the HFD-induced
361 exacerbation of OA-like changes in SAMP8. Although it has been reported that
362 apoptosis often plays an important role in OA pathogenesis, apoptosis can be both a
363 cause and a consequence of OA[24]. Our recent study showed that chondrocyte
364 apoptosis in SAMP8 did not increase up to 11 weeks of age[9]. Moreover, both
365 mechanical stress and HFD independently provoke chondrocyte apoptosis by inducing
366 ER stress[22, 47]. The accumulation of mechanical stress or free fatty acids (FFAs),
367 which are consequences of HFD-induced obesity, triggers ER stress in
368 chondrocytes[22, 23, 47, 48]. Under excessive ER stress, apoptotic pathways will be
369 activated primarily via CHOP[49]. The deletion of CHOP in mice has been shown to
370 inhibit chondrocyte apoptosis and reduce the severity of OA in a surgical model[50].
371 The ER stress-induced rise of CHOP activates a series of pro-apoptotic molecules,
372 leading to the upregulation of apoptosis and, eventually, exacerbates OA
373 progression[22, 47]. Indeed, excessive ER stress might be involved in apoptotic
374 pathways because CHOP was increased in articular chondrocytes of HFD-fed SAMP8.
375 As a limitation of the present study, although we did not clarify the main factors that
376 induce chondrocyte apoptosis in HFD-fed SAMP8, it suggests that apoptosis via
377 increased mechanical stress, accumulation of excessive FFAs, and waste products
378 from liver, such as ammonia, might be a potential mechanism that accelerated severity
379 of OA in HFD-fed SAMP8.

Together, our study demonstrated that HFD feeding further promotes the spontaneous OA progression via obesity with liver damage in SAMP8 at 14 weeks of age. Chondrocyte apoptosis is a potential mechanism underlying the promotion of OA development by HFD in SAMP8. These findings can be useful to better understand the mechanisms between aging, obesity and OA.

Abbreviations

OA: osteoarthritis; SAMP8: Senescence-Accelerated Mouse-Prone 8; BMD: bone mineral density; DAPI: 4′,6-diamidino-2-phenylindole;

Declarations

Ethics approval and consent to participate

All animal experiments were performed according to protocols approved by the institutional Animal Care and Use Committees at Hiroshima University.

Availability of data and materials

The datasets used and/or analyzed during the current study are available from the corresponding author on request.

Competing interests

The authors declare no competing interests.

Funding

This research was supported by MEXT/JPS KAKENHI for Grant-in-Aid for Scientific Research (B) Grant 15H04959 (SM), Mitsui Sumitomo Insurance Welfare Foundation (SM). The study sponsors had no role in the study design, collection, analysis and interpretation of data; the writing of the manuscript; or the decision to submit the manuscript for publication.

Author contributions

C.D and S.M contributed to the conception and design of the study. C.D, D.Y, Y.M and Y.S performed the experiments. C.D, T.N, K.M, N.A and S.M contribute to the analysis and interpretation of data. C.D and S.M contributed to draft manuscript. All authors approved the submitted manuscript.

Acknowledgements

We thank T. Miyata, E. Ueda, DVM., M. A. Saito and Y. Takagi for excellent technical support, and M. Miyaki, DVM. Ph.D. for statistical analysis. A part of this work was carried out at the Analysis Center of Life Science, Natural Science Center for Basic Research and Development, Hiroshima University.

References

1. Hunter DJ, Bierma-Zeinstra S. Osteoarthritis. The Lancet. 2019;393(10182):1745-59.
2. Long H, Liu Q, Yin H, Wang K, Diao N, Zhang Y, et al. Prevalence Trends of Site‐Specific Osteoarthritis From 1990 to 2019: Findings From the Global Burden of Disease Study 2019. Arthritis & Rheumatology. 2022;74(7):1172-83.
3. Thijssen E, van Caam A, van der Kraan PM. Obesity and osteoarthritis, more than just wear and tear: pivotal roles for inflamed adipose tissue and dyslipidaemia in obesity-induced osteoarthritis. Rheumatology (Oxford). 2015;54(4):588-600.
4. Losina E, Weinstein AM, Reichmann WM, Burbine SA, Solomon DH, Daigle ME, et al. Lifetime risk and age at diagnosis of symptomatic knee osteoarthritis in the US. Arthritis Care Res (Hoboken). 2013;65(5):703-11.
5. Takeda T, Hosokawa M, Higuchi K. Senescence-accelerated mouse (SAM): a novel murine model of senescence. Experimental Gerontology. 1997;32(1-2):105-9.
6. Takeda T. Senescence-accelerated mouse (SAM) with special references to neurodegeneration models, SAMP8 and SAMP10 mice. Neurochem Res. 2009;34(4):639-59.
7. Miyaki S, Sato T, Inoue A, Otsuki S, Ito Y, Yokoyama S, et al. MicroRNA-140 plays dual roles in both cartilage development and homeostasis. Genes Dev. 2010;24(11):1173-85.
8. Takada T, Miyaki S, Ishitobi H, Hirai Y, Nakasa T, Igarashi K, et al. Bach1 deficiency reduces severity of osteoarthritis through upregulation of heme oxygenase-1. Arthritis Res Ther. 2015;17:285.
9. Sanada Y, Ikuta Y, Ding C, Shinohara M, Yimiti D, Ishitobi H, et al. Senescence-accelerated mice prone 8 (SAMP8) in male as a spontaneous osteoarthritis model. Arthritis Res Ther. 2022;24(1):235.
10. Griffin TM, Huebner JL, Kraus VB, Guilak F. Extreme obesity due to impaired leptin signaling in mice does not cause knee osteoarthritis. Arthritis Rheum. 2009;60(10):2935-44.
11. Berenbaum F, Griffin TM, Liu-Bryan R. Review: Metabolic Regulation of Inflammation in Osteoarthritis. Arthritis & Rheumatology. 2017;69(1):9-21.
12. Sansone V, Applefield RC, De Luca P, Pecoraro V, Gianola S, Pascale W, et al. Does a high-fat diet affect the development and progression of osteoarthritis in mice?: A systematic review. Bone Joint Res. 2019;8(12):582-92.
13. Guss JD, Ziemian SN, Luna M, Sandoval TN, Holyoak DT, Guisado GG, et al. The effects of metabolic syndrome, obesity, and the gut microbiome on load-induced osteoarthritis. Osteoarthritis Cartilage. 2019;27(1):129-39.
14. Min Y, Ahn D, Truong TMT, Kim M, Heo Y, Jee Y, et al. Excessive sucrose exacerbates high fat diet-induced hepatic inflammation and fibrosis promoting osteoarthritis in mice model. J Nutr Biochem. 2023;112:109223.
15. Glasson SS, Chambers MG, Van Den Berg WB, Little CB. The OARSI histopathology initiative - recommendations for histological assessments of osteoarthritis in the mouse. Osteoarthritis Cartilage. 2010;18 Suppl 3:S17-23.
16. Nagira K, Ikuta Y, Shinohara M, Sanada Y, Omoto T, Kanaya H, et al. Histological scoring system for subchondral bone changes in murine models of joint aging and osteoarthritis. Sci Rep. 2020;10(1):10077.
17. Kwok J, Onuma H, Olmer M, Lotz MK, Grogan SP, D'Lima DD. Histopathological analyses of murine menisci: implications for joint aging and osteoarthritis. Osteoarthritis Cartilage. 2016;24(4):709-18.

18. Krenn V, Morawietz L, Haupl T, Neidel J, Petersen I, Konig A. Grading of chronic synovitis--a histopathological grading system for molecular and diagnostic pathology. Pathol Res Pract. 2002;198(5):317-25.
19. Kawai T, Autieri MV, Scalia R. Adipose tissue inflammation and metabolic dysfunction in obesity. Am J Physiol Cell Physiol. 2021;320(3):C375-C91.
20. Quail DF, Dannenberg AJ. The obese adipose tissue microenvironment in cancer development and progression. Nat Rev Endocrinol. 2019;15(3):139-54.
21. Guo AY, Leung KS, Siu PM, Qin JH, Chow SK, Qin L, et al. Muscle mass, structural and functional investigations of senescence-accelerated mouse P8 (SAMP8). Exp Anim. 2015;64(4):425-33.
22. Tan L, Harper L, McNulty MA, Carlson CS, Yammani RR. High-fat diet induces endoplasmic reticulum stress to promote chondrocyte apoptosis in mouse knee joints. Faseb j. 2020;34(4):5818-26.
23. Tan L, Yammani RR. Nupr1 regulates palmitate-induced apoptosis in human articular chondrocytes. Biosci Rep. 2019;39(2).
24. Hwang HS, Kim HA. Chondrocyte Apoptosis in the Pathogenesis of Osteoarthritis. Int J Mol Sci. 2015;16(11):26035-54.
25. Diekman BO, Sessions GA, Collins JA, Knecht AK, Strum SL, Mitin NK, et al. Expression of p16(INK)(4a) is a biomarker of chondrocyte aging but does not cause osteoarthritis. Aging Cell. 2018;17(4):e12771.
26. Svensson AM, Hellerström C, Jansson L. Diet-induced obesity and pancreatic islet blood flow in the rat: a preferential increase in islet blood perfusion persists after withdrawal of the diet and normalization of body weight. J Endocrinol. 1996;151(3):507-11.
27. Izquierdo V, Palomera-Avalos V, Pallas M, Grinan-Ferre C. Resveratrol Supplementation Attenuates Cognitive and Molecular Alterations under Maternal High-Fat Diet Intake: Epigenetic Inheritance over Generations. Int J Mol Sci. 2021;22(3).
28. Rui Y, Lv M, Chang J, Xu J, Qin L, Wan Z. Chia Seed Does Not Improve Cognitive Impairment in SAMP8 Mice Fed with High Fat Diet. Nutrients. 2018;10(8).
29. Evans AL, Paggiosi MA, Eastell R, Walsh JS. Bone density, microstructure and strength in obese and normal weight men and women in younger and older adulthood. J Bone Miner Res. 2015;30(5):920-8.
30. Sanchez-Lopez E, Coras R, Torres A, Lane NE, Guma M. Synovial inflammation in osteoarthritis progression. Nat Rev Rheumatol. 2022;18(5):258-75.
31. Ionova-Martin SS, Do SH, Barth HD, Szadkowska M, Porter AE, Ager JW, 3rd, et al. Reduced size-independent mechanical properties of cortical bone in high-fat diet-induced obesity. Bone. 2010;46(1):217-25.
32. Halade GV, El Jamali A, Williams PJ, Fajardo RJ, Fernandes G. Obesity-mediated inflammatory microenvironment stimulates osteoclastogenesis and bone loss in mice. Exp Gerontol. 2011;46(1):43-52.
33. Marzetti E, Calvani R, Tosato M, Cesari M, Di Bari M, Cherubini A, et al. Sarcopenia: an overview. Aging Clin Exp Res. 2017;29(1):11-7.
34. Pegreffi F, Balestra A, De Lucia O, Smith L, Barbagallo M, Veronese N. Prevalence of Sarcopenia in Knee Osteoarthritis: A Systematic Review and Meta-Analysis. J Clin Med. 2023;12(4).
35. Ye X, Meeker HC, Kozlowski PB, Wegiel J, Wang KC, Imaki H, et al. Pathological changes in the liver of a senescence accelerated mouse strain (SAMP8): a mouse model for the study of liver diseases. Histol Histopathol. 2004;19(4):1141-51.

36. Ito M, Suzuki J, Tsujioka S, Sasaki M, Gomori A, Shirakura T, et al. Longitudinal analysis of murine steatohepatitis model induced by chronic exposure to high-fat diet. Hepatol Res. 2007;37(1):50-7.
37. Wu Y, Wu T, Wu J, Zhao L, Li Q, Varghese Z, et al. Chronic inflammation exacerbates glucose metabolism disorders in C57BL/6J mice fed with high-fat diet. J Endocrinol. 2013;219(3):195-204.
38. Asokan SM, Wang T, Wang MF, Lin WT. A novel dipeptide from potato protein hydrolysate augments the effects of exercise training against high-fat diet-induced damages in senescence-accelerated mouse-prone 8 by boosting pAMPK / SIRT1/ PGC-1α/ pFOXO3 pathway. Aging (Albany NY). 2020;12(8):7334-49.
39. Han AL. Association between metabolic associated fatty liver disease and osteoarthritis using data from the Korean national health and nutrition examination survey (KNHANES). Inflammopharmacology. 2021;29(4):1111-8.
40. Zhuo Q, Yang W, Chen J, Wang Y. Metabolic syndrome meets osteoarthritis. Nat Rev Rheumatol. 2012;8(12):729-37.
41. Heydemann A. An Overview of Murine High Fat Diet as a Model for Type 2 Diabetes Mellitus. J Diabetes Res. 2016;2016:2902351.
42. De Chiara F, Thomsen KL, Habtesion A, Jones H, Davies N, Gracia-Sancho J, et al. Ammonia Scavenging Prevents Progression of Fibrosis in Experimental Nonalcoholic Fatty Liver Disease. Hepatology. 2020;71(3):874-92.
43. Zhou HW, Lou SQ, Zhang K. Recovery of function in osteoarthritic chondrocytes induced by p16INK4a-specific siRNA in vitro. Rheumatology (Oxford). 2004;43(5):555-68.
44. Jeon OH, Kim C, Laberge RM, Demaria M, Rathod S, Vasserot AP, et al. Local clearance of senescent cells attenuates the development of post-traumatic osteoarthritis and creates a pro-regenerative environment. Nat Med. 2017;23(6):775-81.
45. Li H, Wang D, Yuan Y, Min J. New insights on the MMP-13 regulatory network in the pathogenesis of early osteoarthritis. Arthritis Res Ther. 2017;19(1):248.
46. Jiang L, Lin J, Zhao S, Wu J, Jin Y, Yu L, et al. ADAMTS5 in Osteoarthritis: Biological Functions, Regulatory Network, and Potential Targeting Therapies. Front Mol Biosci. 2021;8:703110.
47. Huang Z, Zhou M, Wang Q, Zhu M, Chen S, Li H. Mechanical and hypoxia stress can cause chondrocytes apoptosis through over-activation of endoplasmic reticulum stress. Arch Oral Biol. 2017;84:125-32.
48. Nazli SA, Loeser RF, Chubinskaya S, Willey JS, Yammani RR. High fat-diet and saturated fatty acid palmitate inhibits IGF-1 function in chondrocytes. Osteoarthritis Cartilage. 2017;25(9):1516-21.
49. Hu H, Tian M, Ding C, Yu S. The C/EBP Homologous Protein (CHOP) Transcription Factor Functions in Endoplasmic Reticulum Stress-Induced Apoptosis and Microbial Infection. Front Immunol. 2018;9:3083.
50. Uehara Y, Hirose J, Yamabe S, Okamoto N, Okada T, Oyadomari S, et al. Endoplasmic reticulum stress-induced apoptosis contributes to articular cartilage degeneration via C/EBP homologous protein. Osteoarthritis Cartilage. 2014;22(7):1007-17.

545 **Figure Legends**

546 **Figure 1. Alterations in body parameters of SAMP8 subjected to HFD feeding.** A)
547 Schematic diagram of the experimental design. B) Monitoring of body weight changes
548 during the experimental timeframe from 5 to 14 weeks of age (n=20 per group). C)
549 Representative images of ND- and HFD-fed SAMP8 at 14 weeks of age prior to
550 sacrifice. D) Liver tissue weights obtained post-sacrifice (n=14 per group). E)
551 Combined weight of epididymal and subcutaneous adipose tissues and their proportion
552 of total body mass (n=14 per group). Data represented as mean ± S.D. Comparison of
553 mean values was performed using 2-way ANOVA with Sidak's multiple correction (body
554 weight) or Welch's t test. *p<0.05, **p<0.01, ***p<0.001. iGTT: intraperitoneal glucose
555 tolerance test.

556

557 **Figure 2. Metabolic alterations in SAMP8 following HFD feeding.** A)
558 Representative images of liver H&E staining. B) Serum levels of liver damage markers
559 aspartate transaminase (AST) and alanine transaminase (ALT) (n=16 per group). C)
560 Serum levels of circulating lipids triglyceride (TG) and total cholesterol (T-CHO) (n=16
561 per group). D) Representative images of H&E-stained epididymal adipose tissue. E)
562 Adipocyte areas in epididymal adipose tissue (n=3 per group). F) Ratio of crown-like
563 structures (CLSs) to adipocytes in epididymal adipose tissue (n=3 per group). G)
564 Changes in blood glucose levels during intraperitoneal glucose tolerance test (iGTT)
565 (left) and area-under-curve of blood glucose (right) (n=12 per group). H) Fasting

566 glucose and non-esterified fatty acid (NEFA) concentrations in serum (n=16 per group).
567 Data represented as mean ± S.D. Comparison of mean values was performed using
568 Welch's t test. *p<0.05, **p<0.01. ns: non-significant difference.
569
570 **Figure 3. Histopathological assessment of knee OA progression in HFD-fed**
571 **SAMP8.** A) Representative images of knee joint safranin O staining. a) and e): articular
572 cartilage; b) and f): medial meniscus; c) and g): synovium (arrowheads); d) and h):
573 subchondral bone of medial tibia. B) Histopathological OARSI scores for entire knee
574 joint cartilage at 14weeks of age (n=20 per group). C) OARSI scores of medial and
575 lateral tibial/femoral cartilage. D) Medial and lateral meniscus scores for left knees
576 (n=20 per group). E) Synovitis scores of left knees (n=20 per group). F) Scores of
577 subchondral bone sclerosis for medial tibias of left knees (n=20 per group). Scoring
578 data represented as median with 95% confidence interval and were compared
579 between ND and HFD groups by Mann–Whitney U test. *p<0.05, **p<0.01, ***p<0.001,
580 ****p<0.0001. ns: non-significant difference.
581
582 **Figure 4. Evaluation of bone density and muscle strength in HFD-fed SAMP8.** A)
583 Bone mineral density of right femurs in ND- and HFD-fed SAMP8 (n=8 per group). B)
584 muscle strength assessment in ND- and HFD-fed SAMP8 using grip strength test
585 (n=20 per group). Data represented as mean ± S.D. Comparison of mean values was
586 performed using multiple unpaired t tests with Holm-Sidak's multiple correction (bone

587 mineral density) or Welch's t test (muscle strength). ns: non-significant difference.

588

589 **Figure 5. In situ staining of potential regulatory markers for OA.** A) TUNEL staining
590 was performed to assess knee joints. (n=8 per group). Green: TUNEL-positive cells;
591 Blue: DAPI nuclear stain. Immunohistochemistry of B) C/EBP homologous protein
592 (CHOP) (n=8 per group), C) $p16^{INK4a}$ (n=8 per group), D) MMP13 (n=8 per group) and
593 E) ADAMTS5 (n=8 per group) were performed and assessed on ND- or HFD-fed
594 SAMP8. Quantification by positive cell number/total cell number were represented as
595 mean ± S.D. Comparison of mean values was performed using Welch's t test. ***p*<0.01.
596 ****p<0.0001. ns: non-significant difference.

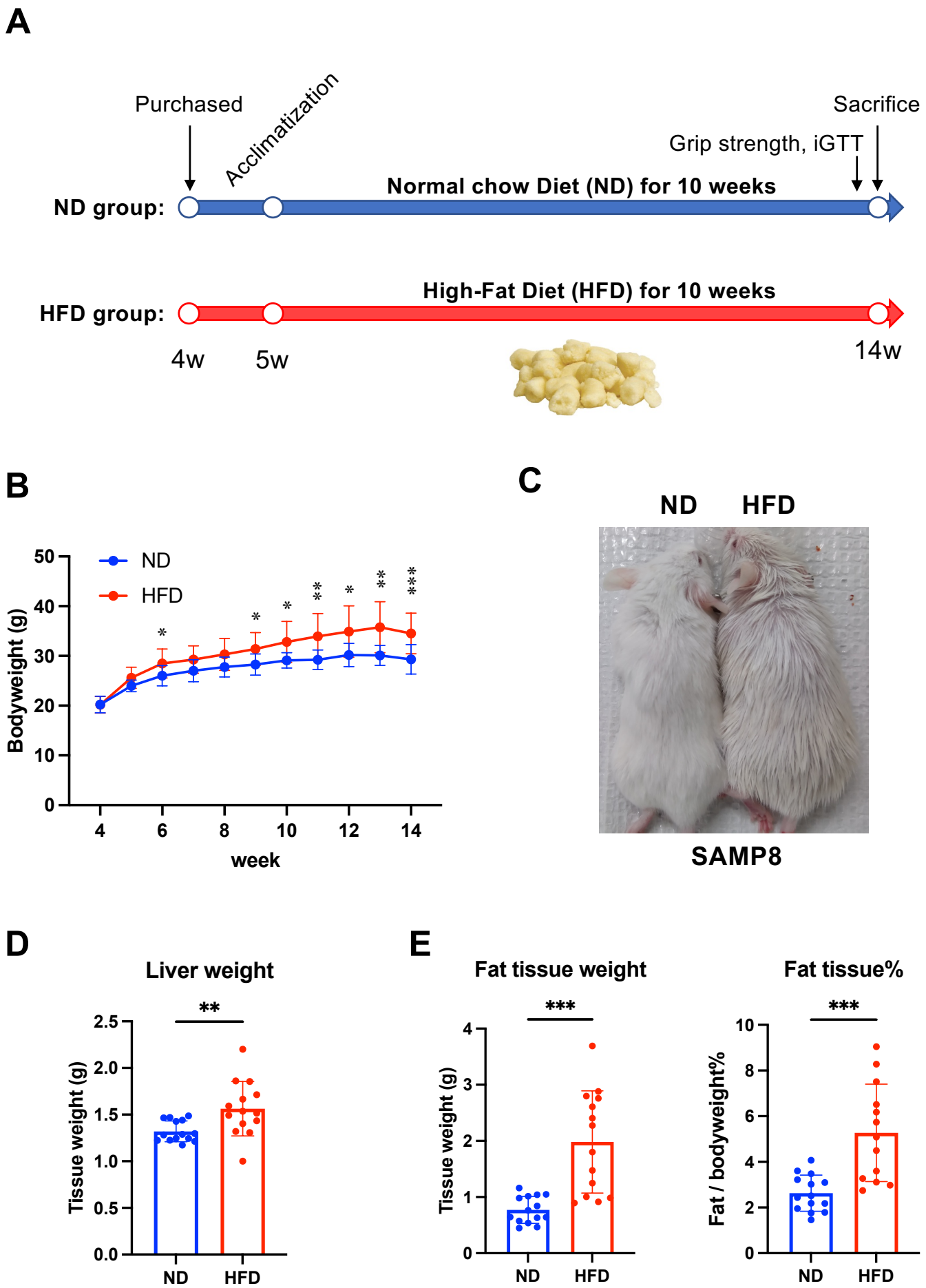
A
Purchased
Acclimatization
Sacrifice
Grip strength, iGTT
ND group:
Normal chow Diet (ND) for 10 weeks
HFD group:
High-Fat Diet (HFD) for 10 weeks
4w
5w
14w
B
ND
HFD
Bodyweight (g)
week
C
ND
HFD
SAMP8
D
Liver weight
Tissue weight (g)
ND
HFD
E
Fat tissue weight
Tissue weight (g)
Fat tissue%
Fat / bodyweight%

Figure 1

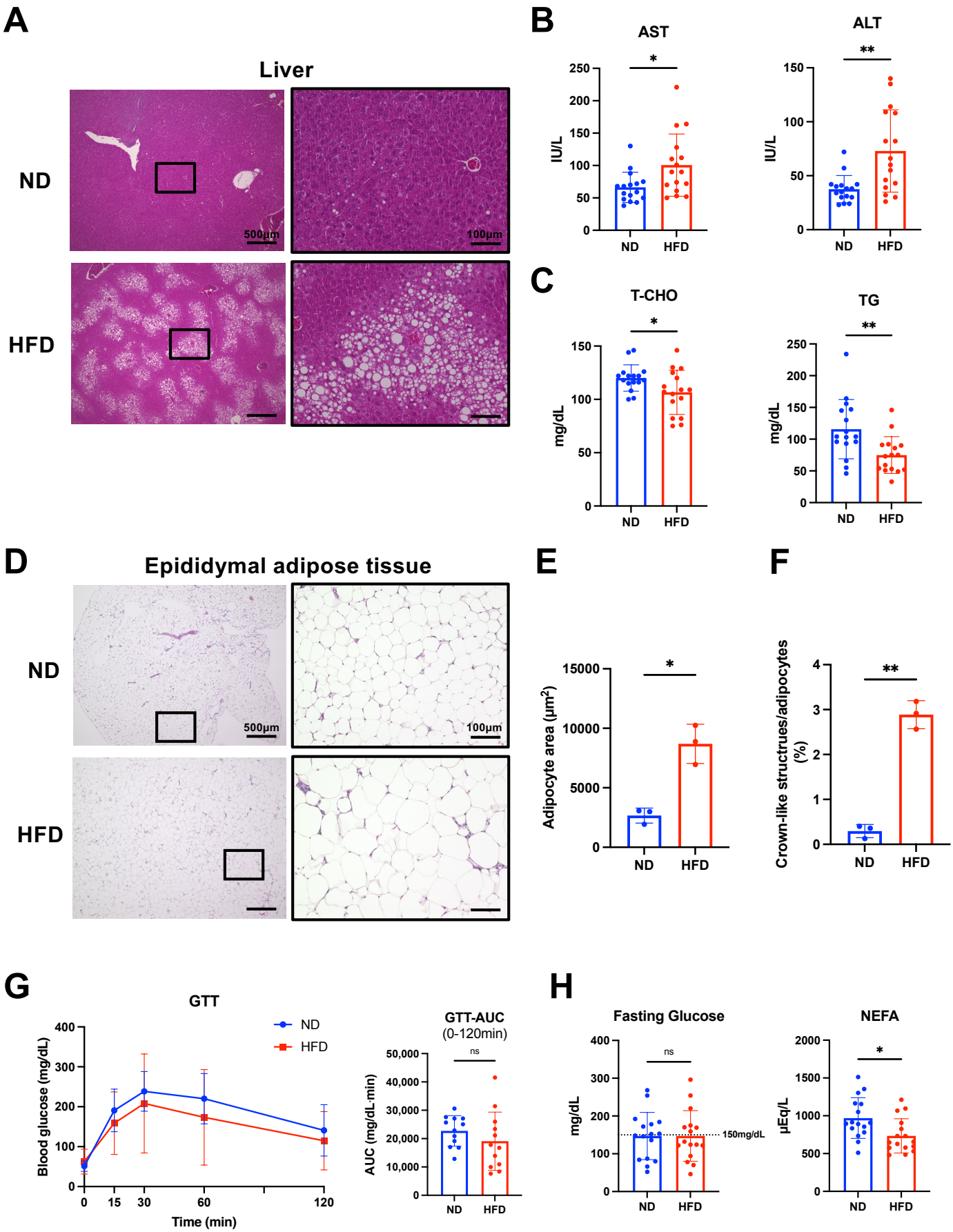
A
Liver
ND
HFD
500μm
100μm
B
AST
ALT
IU/L
ND
HFD
C
T-CHO
TG
mg/dL
D
Epididymal adipose tissue
E
Adipocyte area (μm²)
F
Crown-like structrues/adipocytes (%)
G
GTT
Blood glucose (mg/dL)
Time (min)
GTT-AUC (0-120min)
AUC (mg/dL·min)
ns
H
Fasting Glucose
150mg/dL
NEFA
μEq/L

Figure 2

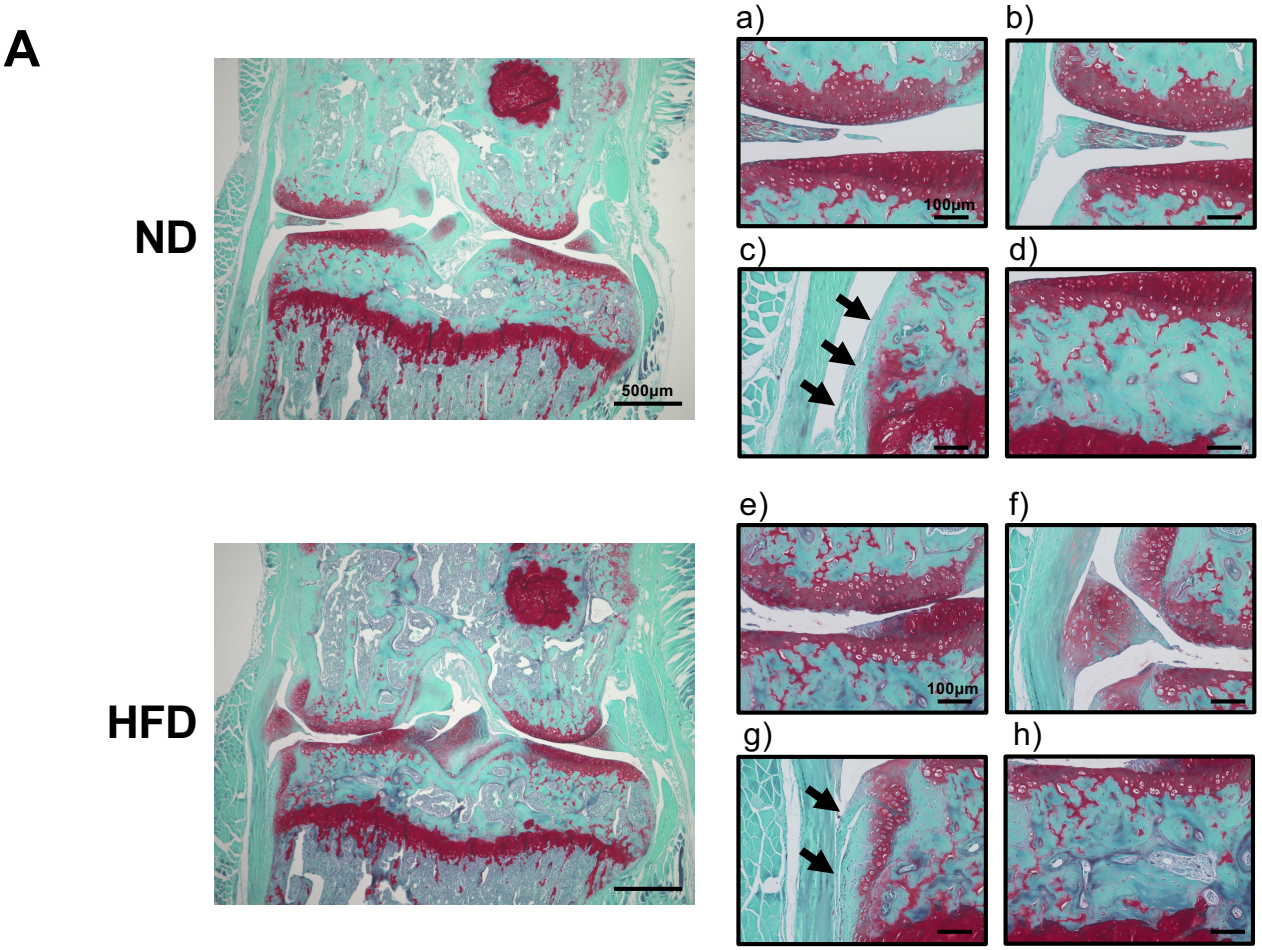
A
ND
HFD
500µm
a)
b)
c)
d)
e)
f)
g)
h)
100µm
100µm

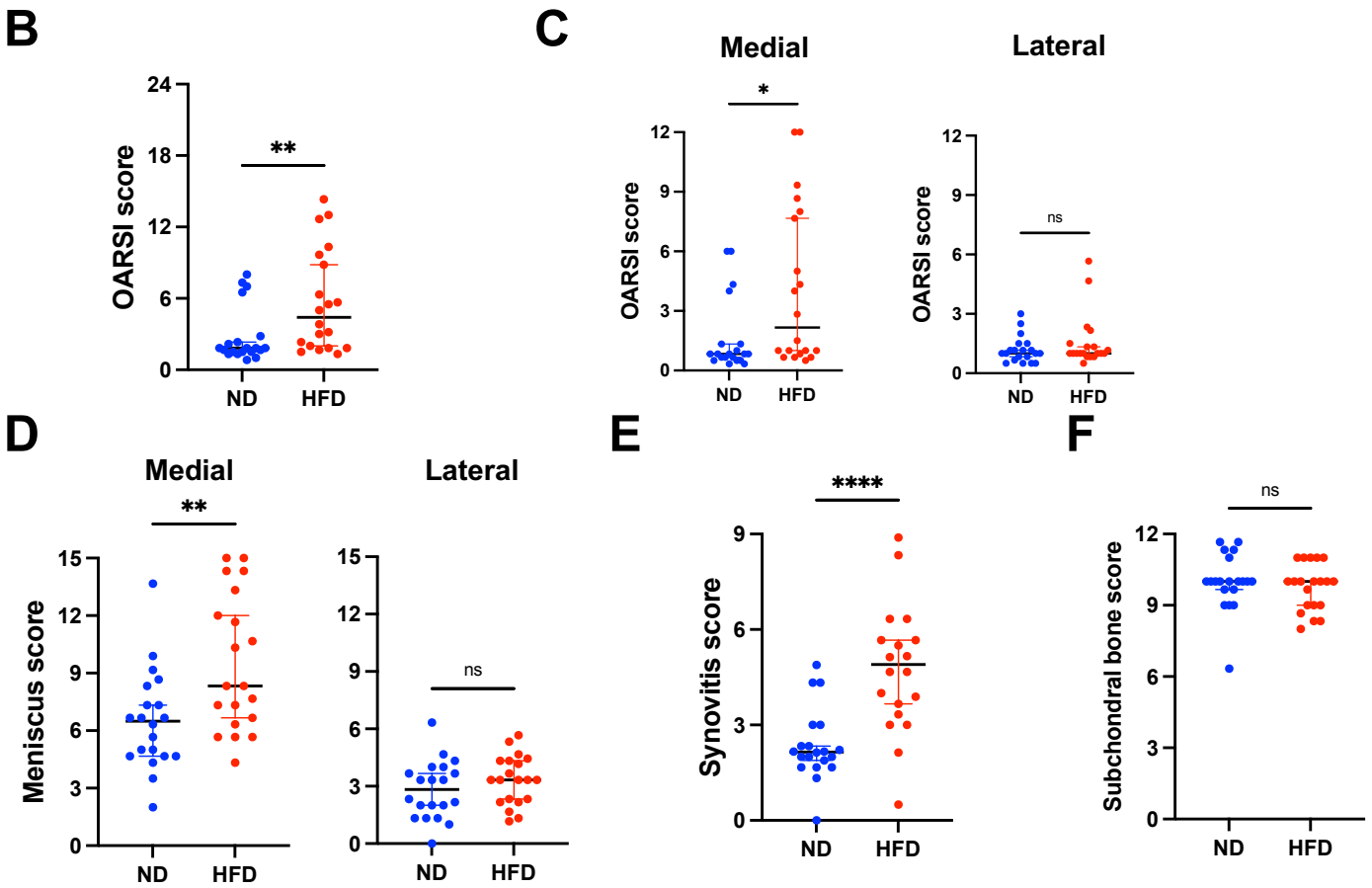
B
OARSI score
24
18
12
6
0
**
ND
HFD
C
Medial
Lateral
OARSI score
12
9
6
3
0
*
ns
ND
HFD
D
Medial
Lateral
Meniscus score
15
12
9
6
3
0
**
ns
ND
HFD
E
Synovitis score
9
6
3
0
****
ND
HFD
F
Subchondral bone score
12
9
6
3
0
ns
ND
HFD

Figure 3

A

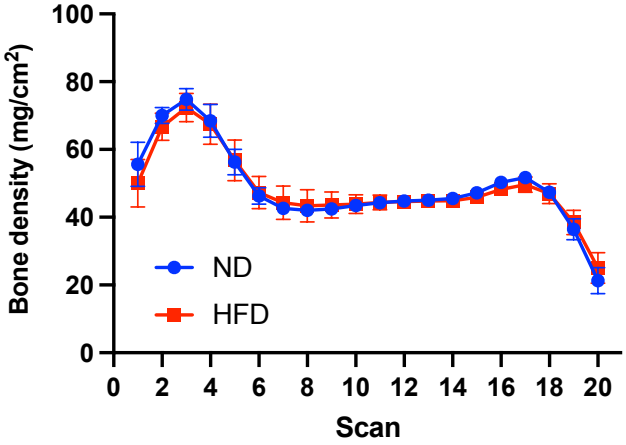
Bone density (mg/cm2)
100
80
60
40
20
0
ND
HFD
0
2
4
6
8
10
12
14
16
18
20
Scan

B

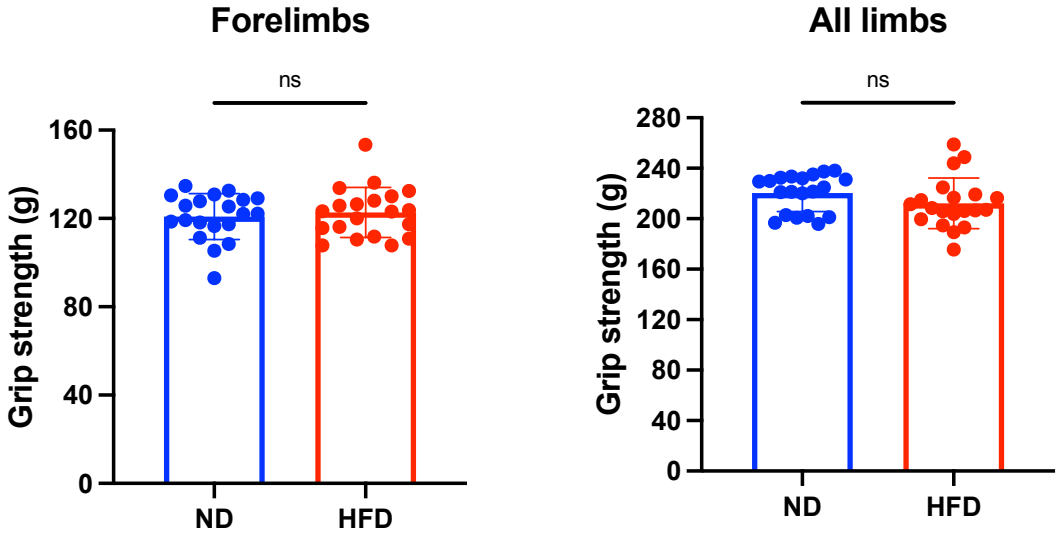
Forelimbs
ns
Grip strength (g)
160
120
80
40
0
ND
HFD
All limbs
ns
Grip strength (g)
280
240
200
160
120
80
40
0
ND
HFD

Figure 4

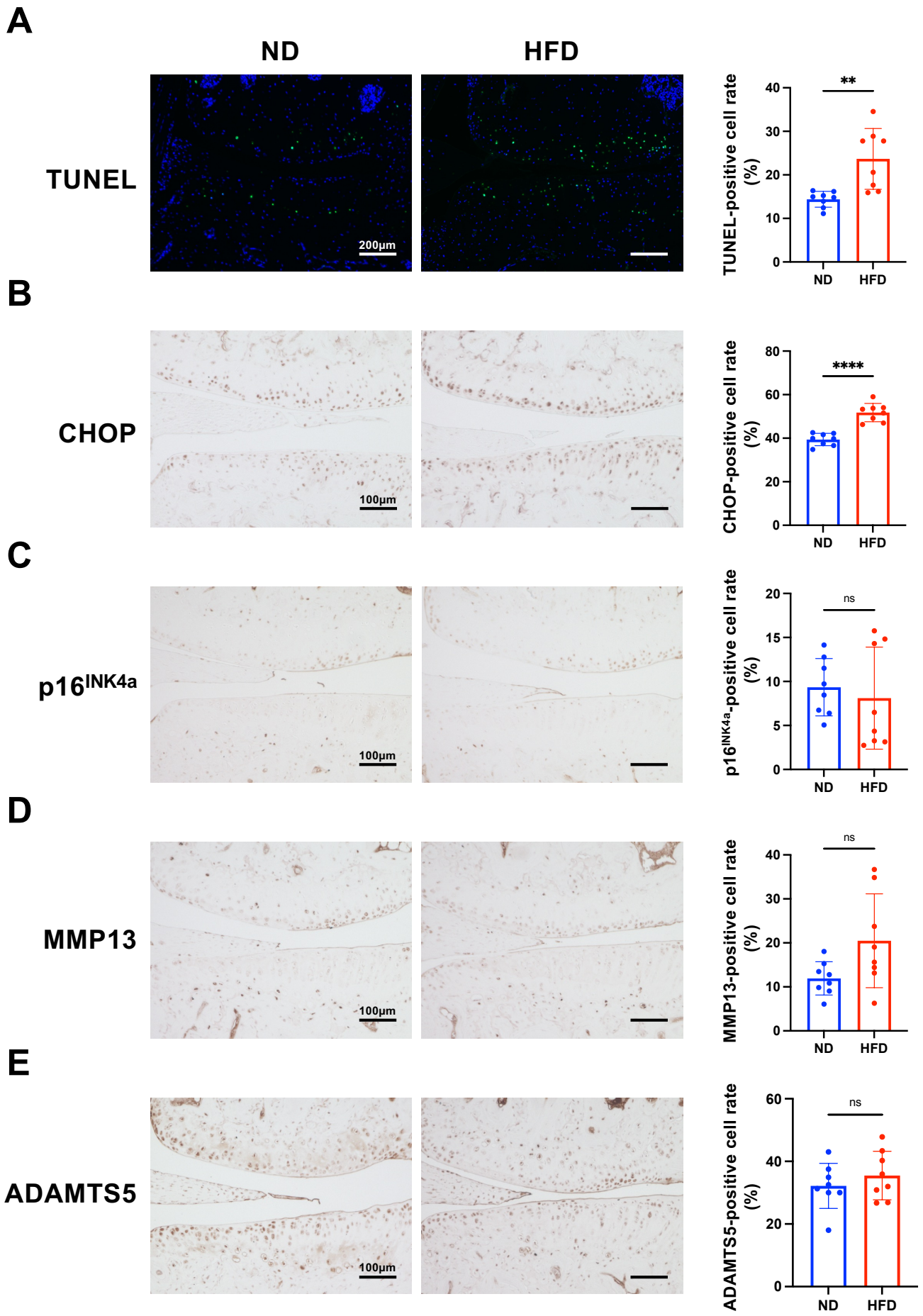
A
ND
HFD
TUNEL
200μm
TUNEL-positive cell rate (%)
**
ND
HFD
B
CHOP
100μm
CHOP-positive cell rate (%)
****
ND
HFD
C
p16INK4a
100μm
p16INK4a-positive cell rate (%)
ns
ND
HFD
D
MMP13
100μm
MMP13-positive cell rate (%)
ns
ND
HFD
E
ADAMTS5
100μm
ADAMTS5-positive cell rate (%)
ns
ND
HFD

Figure 5

Supplemental Materials

Materials and Methods

Glucose Tolerance Test (GTT)

The intraperitoneal glucose tolerance test (iGTT) was performed one day before sacrificing at the end point of the animal study. The SAMP8 underwent fasting for 16 hours prior to the test. The mice were weighed and injected intraperitoneally with 10% D-glucose solution (1.5 g/kg body weight). The blood samples were obtained from the tail veins at 0, 15, 30, 60 and 120 min following the administration and glucose levels were measured using a glucose meter MEDISAFE (TERUMO, Japan).

Dual-energy X-ray Absorptiometry (DEXA) Analysis

The skin and muscles were removed from the right hind limbs which were fixed in 4% PFA-PBS for 48 h at 4°C. Bone mineral density (BMD) in femur bone was measured using dual-energy X-ray absorptiometry (DEXA) densitometry (Aloka DCS600EX, Aloka Co., Tokyo, Japan). Bone density measurements of right femur were taken from sixteen consecutive images with a scan pitch of 2 mm by DEXA scan from the distal femur.

Grip Strength Test

Muscle strength was evaluated by measuring grip strength at 14 weeks of age (MK-380Si; MUROMACHI Kikai Co., Ltd. Japan). The wire mesh was grasped by the forelimb or all limbs of the mouse and pulled backward until it was released. The value

of the spring scale linked to the wire mesh was recorded. The measurement was performed 5 times per mouse, and the average value was used for statistical analysis.

Blood Biochemical Analysis

Blood samples were collected by cardiac puncture after sacrifice. After coagulating at room temperature for one hour, the blood samples were centrifuged under 1,500g for 30 min. Supernatant serum were collected for subsequent analyses. Serum biomarkers of total protein, albumin (ALB), albumin/globulin (A/G) ratio, blood urea nitrogen (BUN), creatinine (CRE) and ammonia (NH_3) in serum were analyzed by Nagahama Life Science Laboratory (Nagahama, Japan) using routine laboratory methods.

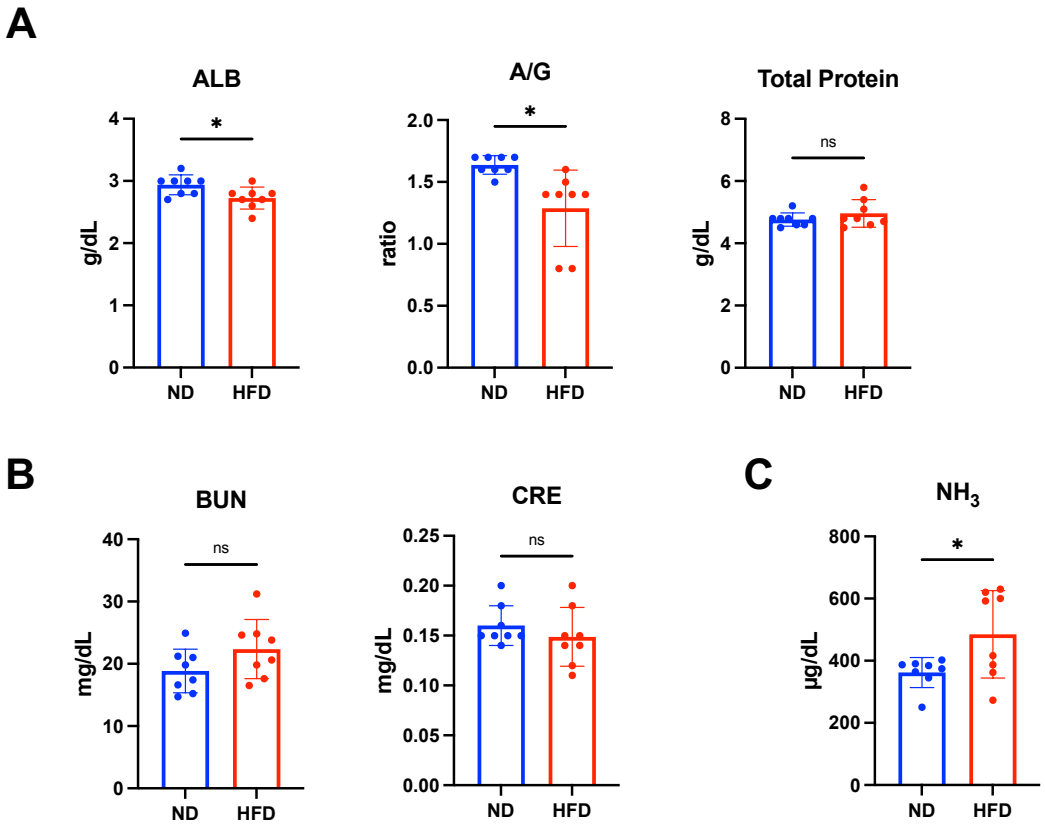

Supplemental Figure 1. Alterations in markers for hepatic and renal function of HFD-fed SAMP8. A) Serum levels of circulating albumin (ALB), albumin/globulin (A/G) ratio and total protein (n=8 per group). B) Serum levels of blood urea nitrogen (BUN) and creatinine (CRE) (n=8 per group). C) Serum levels of ammonia (NH_3) (n=8 per group). Data represented as mean ± S.D. Comparison of mean values was performed using Welch's t test. *p<0.05. ns: non-significant difference.